



Nuclear Materials Authority
P.O.Box 530 Maadi, Cairo, Egypt

ISSN 2314-5609
Nuclear Sciences Scientific Journal
5, 179-195
2016

<http://www.ssnma.com>

GEOLOGY, GEOCHEMISTRY AND MINERALOGY OF YOUNGER GRANITES FROM GABAL RABDI AREA, SOUTH EASTERN DESERT, EGYPT

MOHAMED A. RASHED

Nuclear Materials Authority, Cairo, Egypt

ABSTRACT

The study area consists of metavolcanics and younger gabbros intruded by younger granites and post granitic dykes. The younger granites are represented by monzogranites and syenogranites. Petrographically, monzogranites are composed mainly of quartz, potash feldspars, plagioclase(An_{9-18}), biotite and hornblende, whereas allanite, zircon and opaques (iron oxides and pyrite) are accessories. The syenogranites are composed mainly of potash feldspars, quartz, plagioclase(An_{4-14}), biotite and muscovite. Zircon and opaques (iron oxides and pyrite) are found as accessories.

Geochemically, the monzogranites are considered as I-type, originated from metaluminous calc-alkaline magma and formed under an extensional regime. They are crystallized at temperature $<800^{\circ}C$, with pressure between 2 to 4 kb. The syenogranites are related to A-type, originated from peraluminous calc-alkaline magma. They are post-orogenic, formed under an extensional regime and are crystallized at temperature $<800^{\circ}C$ with pressure from 1 to 3 kb. The monzogranites and syenogranites have high contents of Zr, Y, Rb, Ba and Nb but syenogranites are higher than monzogranites in above contents except Ba. These younger granites are characterized by presence of radioactive mineral (uranophane) in association with columbite, zircon, pyrite and allanite. Spectrometry, the monzogranites have an average content up to 7 ppm eU and 25 ppm eTh. The syenogranites have an average content up to 9 ppm eU and 23 ppm eTh. The radioactive anomaly is related to shear zone in syenogranites (up to 98 ppm eU and 49 ppm eTh). The origin of uranium in the shear zone is epigenetic and related to ascending hydrothermal solutions as well as accumulation of uranium leaching from the surrounding rocks and re-deposited in the shear zone.

INTRODUCTION

The final stage of Neoproterozoic crustal evolution in Egypt is characterized by intrusion of a group of granitic rocks known as younger granitoids (Akaad and Noweir, 1980; El Gaby et al., 1990). These granitoids constitute a major component of the crust in the Eastern Desert of Egypt. They range in composition from granodiorite to granite with I-type characteristics, but have some A-type affinities (Stern and Hedge, 1985; Abdel-Rahman and Martin, 1990.).

The Precambrian basement rocks of the Eastern Desert of Egypt are characterized by abundant granitoid rocks of wide compositional variations. El-Gaby and Habib, (1982) classified the Pan-African granites into: *i*) Calc-alkaline subduction-related granite series comprising: *a*) the syn-orogenic older granitoid; and *b*) the late orogenic, two feldspar younger pink granites; and *ii*) Alkaline to peralkaline anorogenic granite series. On the other hand Noweir et al.,(1990), classified the Egyptian granitoid rocks into: *i*) syn- to late orogenic older granitoid assemblages (880-

610 Ma) emplaced during the mature intra-oceanic island-arc stage (Ragab et al., 1989); and *ii*) post-orogenic to anorogenic younger granitoid assemblages (600-475 Ma). Most of the post-tectonic younger granites are K- and LILE-enriched, calc-alkaline to mildly alkaline rocks with I-type affinity. A part of the younger granites has been recently classified as A-type granitoids (Eby, 1992). Most of Egyptian uranium occurrences (Um Ara, Gattar, Missikat and Erediya) belong to meta-luminous to slightly peraluminous granites (biotite only or biotite with subordinate secondary muscovite, calc-alkaline in nature and equivalent to A-type (Ibrahim, 1996).

The present work deals with geology, geochemistry, mineralogy and spectrometric prospecting of Gabal Rabdi younger granites, South Eastern Desert, Egypt.

GEOLOGIC SETTING

The Gabal Rabdi area lies in the eastern corner of the South Eastern Desert of Egypt at about 20 km south west of Marsa Alam City on the Red Sea Coast (Fig. 1). The study area is located between Lat. $24^{\circ} 55' 28'' - 24^{\circ} 57' 27''$ N and Long. $34^{\circ} 46' 34'' - 34^{\circ} 50' 39''$ E. The study area is covered by metavolcanics (oldest), younger gabbros, younger granites (monzogranites and syenogranites) and post granitic dykes (youngest), (Fig. 2). The metavolcanic rocks occupy the north, west and the south parts of the mapped area and range in composition from acidic to basic ones. These rocks are hard, massive, moderate to high topographic relief. They are grey, brown to black in colors. The younger gabbros occupy the eastern part of Gabal Rabdi with low to moderate topographic relief.

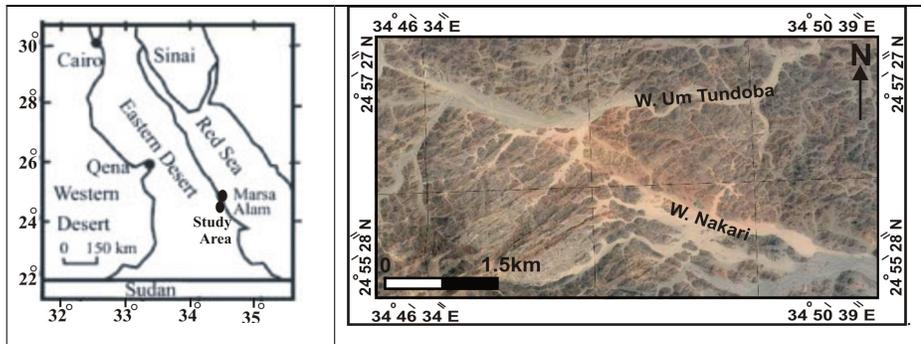


Fig. 1: Location map and Google image for the study area

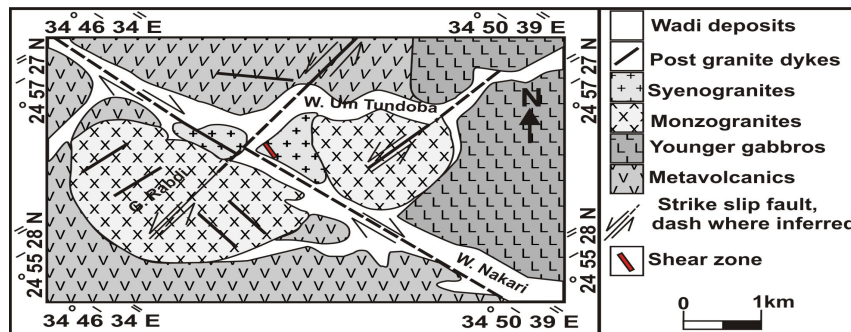


Fig. 2: Geologic map of Gabal Rabdi area, South Eastern Desert, Egypt (Modified after Ali et al., 2005)

These rocks are medium to coarse-grained and dark grey in color (Fig. 3). The granitic rocks occupy the central part of the mapped area and are represented by monzogranites and syenogranites (Fig. 4). The monzogranites show rugged topographic relief with moderate to high peaks. These rocks are medium to coarse grained with light grey color and are highly weathered in some parts forming cavernous shape. These rocks are jointed, fractured and dissected by acidic and basic dykes. The syenogranites occupy a small part in the center of the map and dissected by two major strike slip faults in NW-SE and NE-SW directions. These rocks are found as small masses with low to moderate topographic relief elongated in NW-SE and NE-SW directions. These rocks are fine to medium grained, reddish pink to red in colors, highly jointed, fractured and sheared. These rocks are highly affected by solutions (magmatic and meteoric). This solutions formed some alteration processes such as hematitization which observed in the surface of these rocks and another processes convert the rocks to more friable rocks and lose some components forming porous syenogranites (Fig. 5). These rocks dissected by shear zone in NW-SE direction (Fig. 6). This shear zone is about 50 m in length and about 2 m in width (Fig. 7). The peripheries of the shear zone are dissected by two strike-slip faults



Fig. 3: Photography showing the younger gabbros

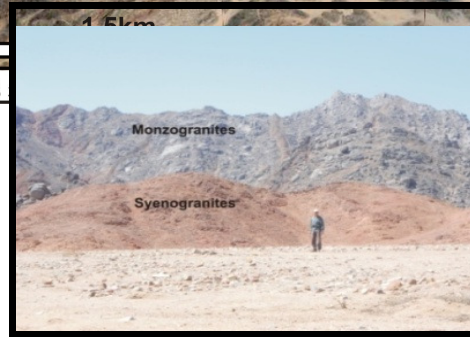


Fig. 4: Photography showing the younger granites represented by monzogranites (grey) and syenogranites (red)



Fig. 5: Photography showing the porous syenogranites



Fig. 6: Photography showing shear zone in NW-SE trending in syenogranites

(dextral). The rocks in this shear zone are fine-grained, sheared and affected by some alteration processes such as hematitization.

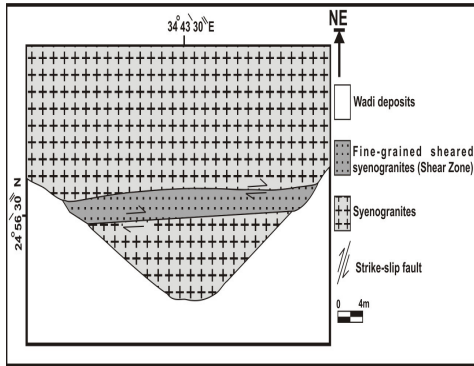


Fig. 7: Sketch showing the syenogranite shear zone.

PETROGRAPHY OF YOUNGER GRANITES

The monzogranites (Table 1 and Fig. 8) are composed of quartz (32.21 vol.%) occurring as subhedral to anhedral crystals and as interstitial grains between feldspar crystals. Few crystals of quartz exhibit undulose extinction. K-feldspar (30.8 vol.%) occurs as subhedral to euhedral crystals and is represented by orthoclase perthite (Fig. 9) of flame and patch-type perthites. Plagioclase (28.1 vol.%) is found as euhedral to subhedral crystals and has albite to oligoclase compo-

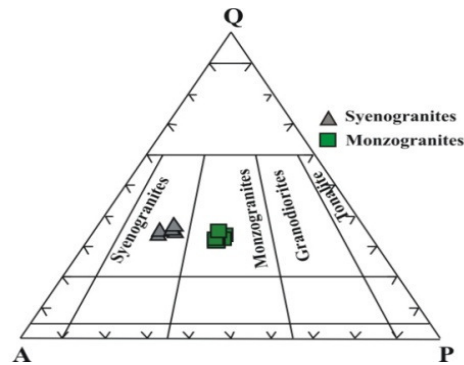


Fig. 8: QAP diagram of younger granites (monzogranites and syenogranites Gabal Rabdi area (After Streckeisen 1976)

sition (An_{9-18}) and exhibits albite and combined albite and pericline twinning. Biotite (3.8 vol.%) occurs as euhedral to subhedral flaky crystals and shows alteration to chlorite. Hornblende (1.8 vol.%) is present as euhedral to subhedral crystals and slightly altered to chlorite. Zircon occurs as semi-prismatic crystals associated with biotite flakes. Allanite occurs as well developed crystals, (Fig.10). Opaques are represented by iron oxides and pyrite as irregular grains scattered throughout the rocks.

Table 1 : Modal analyses of monzogranites and syenogranites from Gabal Rabdi area, South Eastern Desert, Egypt

Rock types	Monzogranites					Syenogranites				
	1	2	3	4	5	6	7	8	9	10
Sample no.										
Quartz	31.5	32.5	33.1	31.5	32.2	33.2	33.4	33.4	34.3	32
K-feldspars	31.1	30.2	30.2	31.2	32.1	44.6	42.2	43.3	42.7	47.7
Plagioclases	29.2	29.5	27.7	27.3	27.3	14.2	17.4	17.3	17	15.1
Mafics	5.7	4.3	6.0	6.5	5.5	3.2	2.9	2.0	2.0	1.5
Opaques	2.0	2.5	2.0	2.0	2.0	2.8	2.1	2.0	2.5	1.5
Accessories+secondary minerals	0.5	1.0	1.0	1.5	1.0	1.0	2.0	2.0	1.5	1.0
Q	34.4	35.3	36.4	37.4	35.2	35.8	35.4	36.2	37.3	34.4
A	33.9	32.6	32.9	32.4	35.2	48.9	45.2	45.7	44.6	50.0
P	31.7	32.1	30.7	30.2	29.6	15.3	19.4	18.1	18.1	15.6

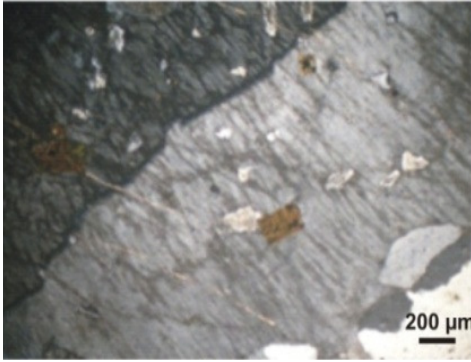


Fig. 9: Photomicrograph showing orthoclase perthite in monzogranites, XPL

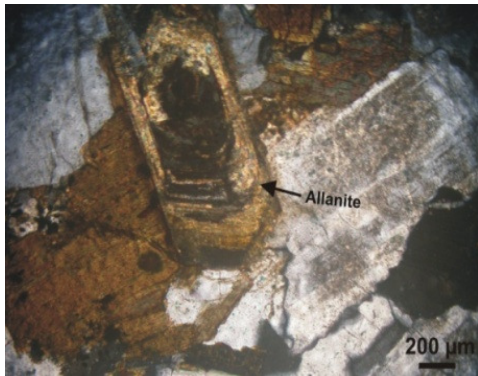


Fig. 10: Photomicrograph showing allanite crystal in monzogranites, XPL

The syenogranites (Table 1 and Fig. 8) consist mainly of k-feldspar (44 vol.%), quartz (33.6 vol. %), plagioclase (16.2 vol. %), biotite and muscovite (2.5 vol.%) . Zircon apatite and opaques, are accessory minerals. Sericite and kaolinite are secondary minerals.

The rock is highly stained by iron oxide solutions appearing as red color on the surface of the rock. K-feldspar are represented by orthoclase perthite showing flame and patch-type of coarse-grained (phenocrysts) (Fig.11). The perthite is highly stained by iron oxide solution appearing along the filling of cleavage by solutions of iron oxides. K-feldspar is altered to kaolinite. Quartz is

present as subhedral, as well as fine crystals, occurring as interstitial grains between the other constituents. The crystals showing wavy to undulose extinction. Plagioclase occurs as subhedral crystals and has albite to oligoclase composition (An. ₄₋₁₄). These crystals are highly fractured and affected by iron oxide solutions along these fractures (Fig. 12). The plagioclase is altered to epidote and zeolite. Biotite occurs as subhedral flakes of faint brown colors. The flakes are highly stained by iron oxide solutions and altered to chlorite and association with muscovite (Fig. 13). Muscovite occurs as subhedral flakes. Zircon occurs as prismatic forms enclosed with biotite (Fig. 14). Opaques represented as iron

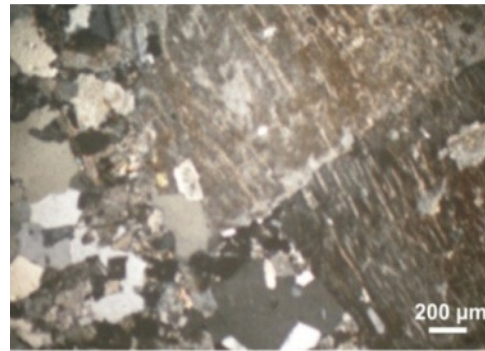


Fig. 11: Photomicrograph showing highly corroded orthoclase perthite in syenogranite, XPL



Fig. 12: Photomicrograph showing cracked plagioclase in syenogranite, XPL

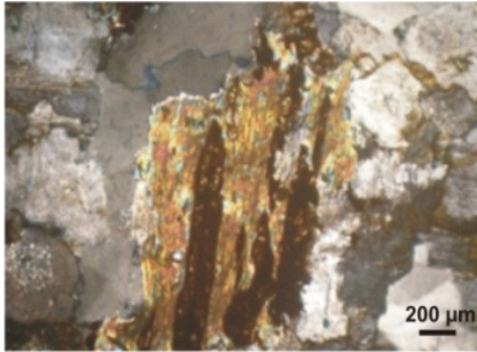


Fig. 13: Photomicrograph showing biotite flakes in association with muscovite in syenogranite, XPL

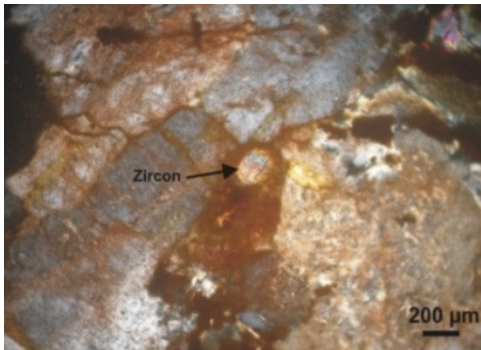


Fig. 14: Photomicrograph showing zircon crystal associated with biotite in syenogranite, XPL

oxides and pyrite and found as abundant grains scattered throughout the rocks.

GEOCHEMISTRY

Twelve samples of younger granites (six from monzogranites and six from syenogranites) were chemically analyzed for major oxides (wt %) by wet chemical methods and trace elements were determined in (ppm) using XRF technique in Nuclear Materials Authority. The results are listed in Table (2)

Geochemical Features of Monzogranites and Syenogranites

From the results of chemical analysis of monzogranites and syenogranites (Table 2),

the monzogranites are relatively high in Al_2O_3 , CaO , Na_2O and MgO relative to syenogranites, while syenogranites are relatively high in SiO_2 and K_2O relative to monzogranites (Fig. 15). Both of the Zr, Y, Rb and Nb contents are relatively higher in syenogranites than monzogranites (Fig. 16).

Geochemical classifications

Based on the normative Ab-Or-An ternary diagram was used by Barker, (1979) as shown in (Fig. 17). On this diagram, the studied samples lie in granite field. The Al_2O_3/Na_2O+K_2O vs. $Al_2O_3/CaO+Na_2O+K_2O$ binary diagram was constructed by Maniar and Piccoli., (1989) to distinguish the different

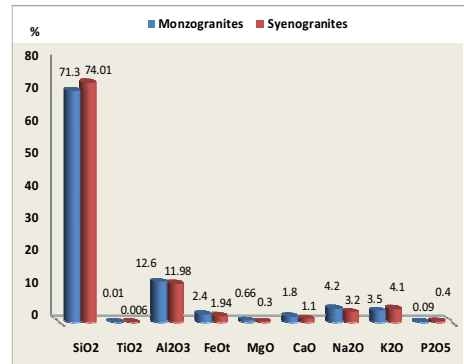


Fig. 15: Histogram showing major oxides (wt. %) for monzogranites and syenogranites

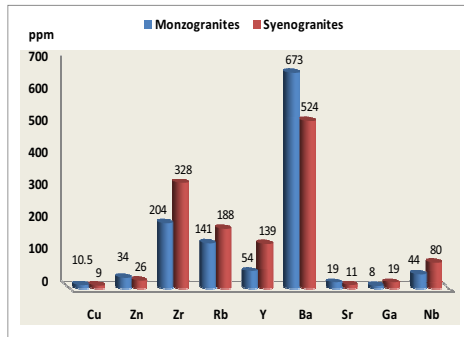


Fig. 16: histogram showing trace elements(ppm) for monzogranites and syenogranites

Table 2: Major oxides(wt%) and trace elements (ppm) of monzogranites and syenogranites from Gabal Rabdi area, South Eastern Desert, Egypt

Sample No.	Monzogranites						Syenogranites					
	1	2	3	4	5	6	7	8	9	10	11	12
SiO ₂	71.9	72.4	70.4	70.18	72.5	70.5	73.4	74.2	74.6	75.8	73.58	72.5
TiO ₂	0.01	0.01	0.01	0.002	0.02	0.01	0.01	0.02	0.002	0.001	0.002	0.001
Al ₂ O ₃	12.3	11.6	13.03	13.5	12.1	13	12.3	12.1	11.1	11.11	12.4	12.9
FeO _i	2.56	2.16	2.4	2.41	2.72	2.3	2.0	2.16	2.56	1.92	1.2	1.84
MgO	1.0	0.8	0.8	0.3	0.3	0.8	0.9	0.2	0.3	0.1	0.2	0.1
CaO	1.9	2.0	1.9	2.2	1.4	1.5	0.9	0.8	1.4	1.0	1.6	0.8
Na ₂ O	4.5	4.2	4.4	3.9	4.01	4.1	3.02	4.0	3.1	3.0	3.0	3.2
K ₂ O	3.8	4.2	3.2	3.4	3.1	3.3	4.1	3.7	3.84	4.2	3.8	4.8
P ₂ O ₅	0.02	0.03	0.03	0.08	0.4	0.03	0.03	0.03	0.03	0.08	0.03	0.04
L.O.I	0.62	0.67	1.98	1.44	1.5	1.9	3	1.61	1.6	1.44	1.78	1.84
Total	98.60	99.07	98.15	97.4	98.05	98.25	99.66	99.12	98.53	98.65	97.59	98.02
ALK	8.3	8.4	7.6	7.3	7.11	7.4	7.12	7.7	6.94	7.2	6.8	8.0
A/CNK	0.82	0.80	0.92	0.93	0.97	0.98	1.11	1.03	0.94	0.98	1.04	1.08
A/Nk	1.07	1.10	1.22	1.28	1.22	1.24	1.31	1.17	1.20	1.17	1.37	1.23

	Trace elements											
	13	9	10	9	12	10	9	9	11	10	9	8
Cu	13	9	10	9	12	10	9	9	11	10	9	8
Zn	23	45	27	34	23	56	25	13	23	34	43	23
Zr	211	232	168	219	237	156	298	299	278	313	318	304
Rb	131	130	153	140	156	137	194	186	167	178	193	213
Y	46	65	78	45	53	42	122	121	158	137	158	138
Ba	666	677	646	695	687	670	577	523	544	532	545	428
Sr	14	13	13	41	16	15	12	9	11	12	11	10
Ga	7	17	6	5	4	9	15	16	22	17	21	22
Nb	37	46	35	65	45	34	80	79	76	87	65	93
Rb/Sr	9.3	10	11.7	3.4	9.75	9.1	16.1	20.6	15.1	14.8	17.5	21.3
Ba/Rb	5	5.2	4.2	4.9	4.4	4.8	2.9	2.8	3.2	2.9	3.4	2.00

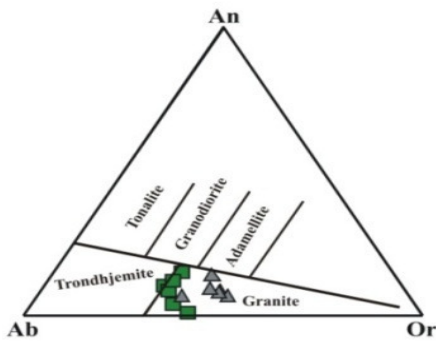


Fig. 17: Normative Ab-Or-An ternary diagram (Barker,1979), for monzogranites and syenogranites of Gabal Rabdi area(symbols as on Fig. 8)

peraluminous, metaluminous and peralkaline magma types. The monzogranite samples fall in the metaluminous field, while the syenogranites samples fall in peraluminous field except two samples fall in metaluminous field (Fig.18).

The K₂O-SiO₂ relationship (Le Maitre, 1989) (Fig. 19) indicates that the studied monzogranites and syenogranites samples plot in the calc-alkaline rock (high k-field). Variation diagram of SiO₂ versus Zr (Newberry et al.,1990) shows that the studied monzogranite samples lie in I-type granite, while syenogranite samples lie in A-type granite (Fig. 20).

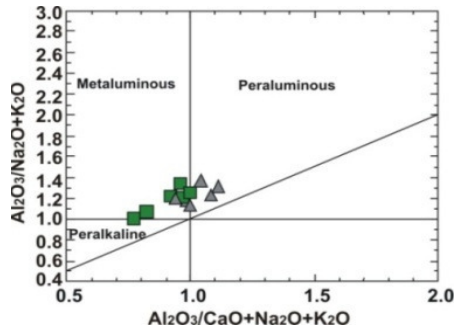


Fig. 18: $Al_2O_3/(Na_2O+K_2O)$ vs. $Al_2O_3/(CaO+Na_2O+K_2O)$ discriminant ion binary diagram (Maniar and Piccoli, 1989) for monzogranites and syenogranites of Gabal Rabdi area

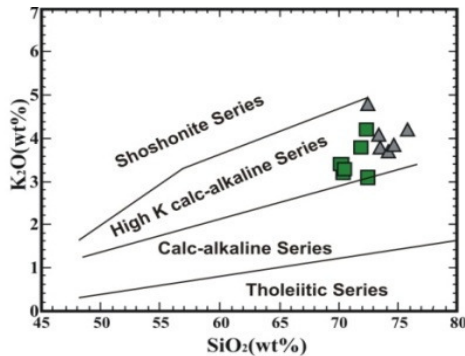


Fig. 19: The K_2O-SiO_2 relationship (Le Maitre 1989), for monzogranites and syenogranites of Gabal Rabdi area

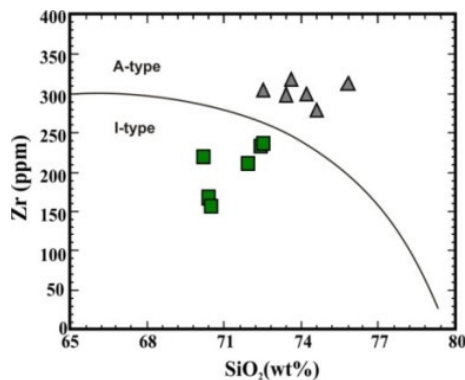


Fig. 20: SiO_2 vs. Zr variation diagram (Newberry et al. 1990), for monzogranites and syenogranites of Gabal Rabdi area

R1-R2 binary diagram (Batchelor and Bowden 1985) shows that the monzogranites samples plot in syn-collision field, while the syenogranites samples plot in post orogenic field (Fig. 21). On AFM ternary diagram of Irvine and Baragar (1971) superimposed by tectonic trends by Petro et al., (1979), the monzogranite and syenogranite samples show tendency to be in the extensional suites (Fig. 22).

According to Ab-An-Or ternary diagram (Tuttle and Bowen 1958), the monzogranites are crystallized at temperature $> 800^\circ C$, with pressure between 2 to 4 kb, while the syenogranites are crystallized at temperature between $760^\circ C$ to $800^\circ C$ with pressure from 1 to 3 kb, (Figs. 23 and 24). Buchanan (1982) suggested that the high Rb/Sr (> 1.5) indicates pre-existing felsic materials in the source rock region, but low Rb/Sr (< 0.7) suggests derivation from the upper mantle. The monzogranites, have an average of Rb/Sr = 9, while in syenogranites the average of Rb/Sr = 17.5, this suggesting presence of felsic materials in their source and were derived from sialic crust. Ba/Rb ratio for granites suggested by Mason, (1966) is 4.1, whereas in the studied monzogranites and syenogranites having Ba/Rb around 4, suggesting that they were derived from sialic crust (Fig. 25).

MINERALOGY

Three samples (10 kg. for each sample) were collected from the shear zone syenogranites and monzogranites. The two samples were crushed to 0.063-0.5 mm size fraction. This size fraction was subjected to systematic mineral separation techniques using heavy liquids (Bromoform, 2.8 sp.gr.), magnetic fractionation using (Frantz Isodynamic Magnetic Separator) and microscopically handpicking mineral grains. Mineral identifications were carried out by X-ray diffraction (XRD) technique. The obtained minerals include:

1-Uranophane ($CaO 2UO_3 2SiO_2 6H_2O$): The uranophane is the radioactive

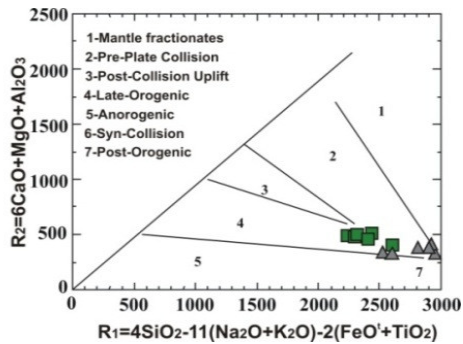


Fig. 21: R1 vs. R2 variation diagram (Batchelor and Bowden, 1985) for monzogranites and syenogranites of Gabal Rabdi area

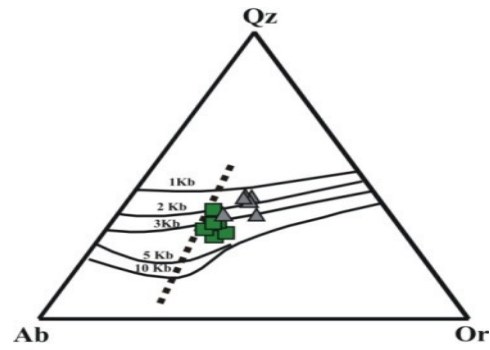


Fig. 24 : Ab-An-Or ternary diagram (Tuttle and Bowen 1958) for monzogranites and syenogranites of Gabal Rabdi area

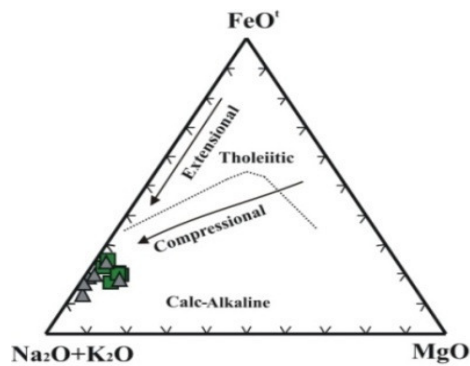


Fig. 22: Na₂O+K₂O-FeO'-MgO ternary diagram (Irvine and Bargar, 1971 and Petro et al. 1979) for monzogranites and syenogranites of Gabal Rabdi area

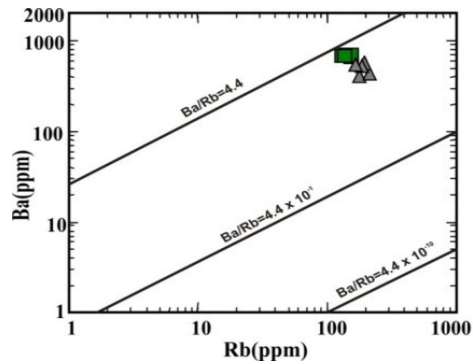


Fig. 25 : Ba vs. Rb binary diagram (Mason 1966) for monzogranites and syenogranites of Gabal Rabdi area

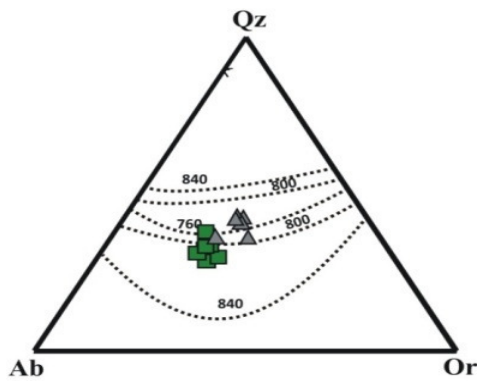


Fig. 23 :Ab-An-Or ternary diagram (Tuttle and Bowen 1958) for monzogranites and syenogranites of Gabal Rabdi area.

mineral recognized in syenogranites shear zone. The grains are soft with canary to pale yellow colors (Fig. 26a and b).

2-Columbite (Fe, Mn)(Nb, Ta)₂O₆: Columbite occurs as well-developed orthorhombic crystals in syenogranites which exhibiting its characteristic black color and shiny white luster (Fig. 27 a and b). Tischendorf, (1977) concluded that columbite mineralization is especially and genetically associated with post-orogenic geochemically distinct granitoids

3- Sulphide minerals; The sulphide minerals are represented as pyrite in monzogranites and syenogranites which occur as skeletal

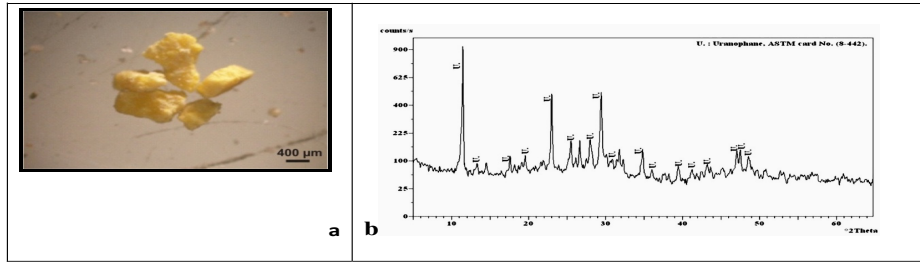


Fig. 26 : a) Soft canary to pale yellow color uranophane and b) X-ray diffractogram for uranophane

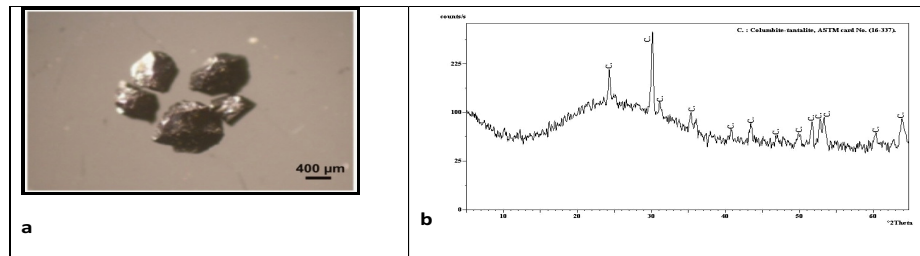


Fig. 27 : a) black color columbite and b) X-ray diffractogram for columbite.

grains of pale-brass yellow in colors (Fig.28 a and b).

4-Zircon ($ZrSiO_4$): The zircon crystals (honey in colors) which occur in monzogranites and syenogranites are represented by short to long prismatic habit (Fig. 29 a and b).

2-Allanite $\{(Ca, Fe^{II})_2(Al, Ce, Fe^{III})_3(SiO_4)_3 \cdot OH\}$: It occurs only in monzogranites as tabular and prismatic crystals of pale brown colors (30a and b).

SPECTROMETRIC PROSPECTING

Normally, Th is three times as abundant as U in natural rocks (Rogers and Adams, 1969). When this ratio is disturbed, it illustrates a depletion or enrichment of uranium. U and Th contents of granitic rocks generally increase during differentiation although in some cases they decrease (Ragland et al., 1967). U/Th ratio can either increase or decrease as it is controlled by the redox conditions, volatile contents, or alteration by endogens or super-

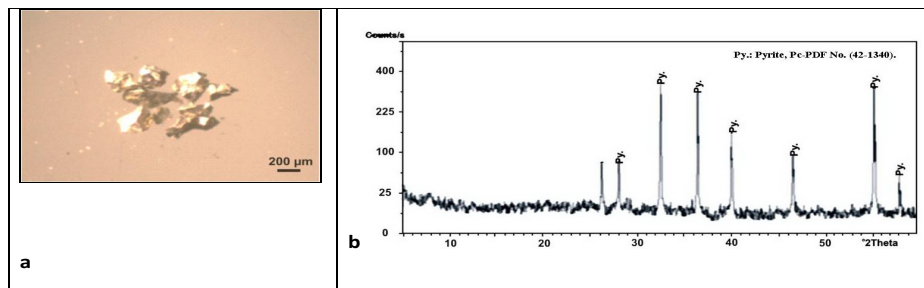


Fig. 28: a) skeletal grains of pale-brass pyrite and b) X-ray diffractogram of pyrite

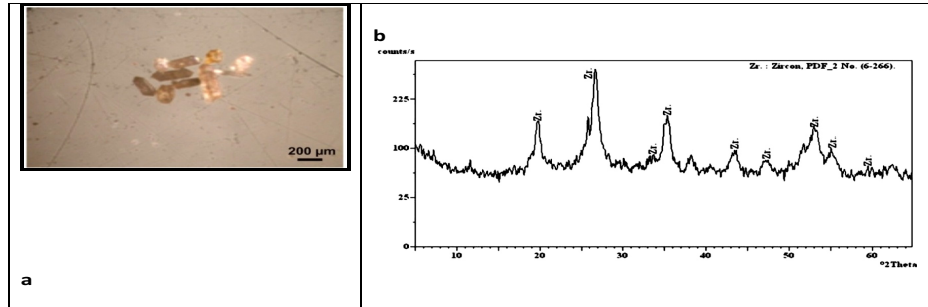


Fig. 29 : a) Short to long prismatic crystals of zircon and b) X-ray diffractogram of zircon

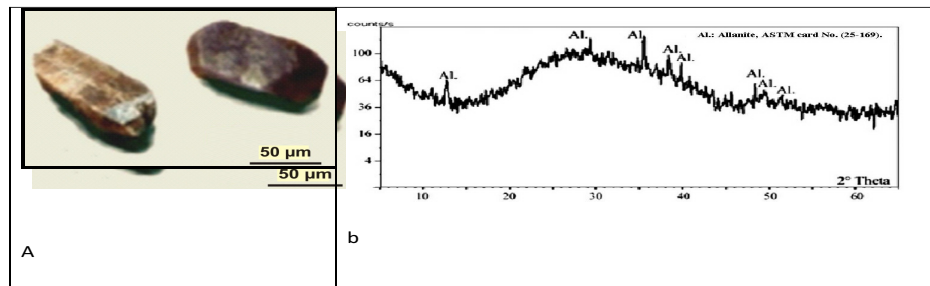


Fig. 30 : a) tabular and long prismatic crystals of allanite and b) X-ray diffractogram of allanite in monzogranites

gene solutions (Falkum and Rose-Hansen, 1978). Relation between uranium and thorium is helpful to test if there is enrichment or depletion of uranium and/or thorium.

The instrument used in the ground γ -ray spectrometric survey measurements is RS-230. Ground γ -ray spectrometric survey can detect dose rate (D.R.) in unit (nanosieverts per hour (nSv h^{-1})), potassium (K%), equivalent uranium content (eU ppm), and equivalent thorium content (eTh ppm). Uranium mobilization (eUm) in the studied rock types can be calculated as follows: the uranium mobilization is calculated difference between the measured eU and the expected original uranium, which is calculated by dividing the measured eTh by the average eTh/eU ratio in the crustal acidic rocks (original uranium = $\text{eTh} / 3.5$ according to Clark et al., 1966) to give the leaching values of uranium ($\text{eUm} = \text{eU} - \text{eTh} / 3.5$). Positive values indicate ura-

nium addition by mobilization, whereas negative values indicated migration of uranium by leaching. D.R., K%, eU, eTh, and other variants of monzogranites, syenogranites, and shear zone are listed in Table 3.

In the monzogranites the eU contents range from 4 to 9 ppm with an average of about 7 ppm. The eTh contents range between 19 to 32 ppm with an average of about 25 ppm. The eU/eTh ratio ranges between 0.19 to 0.33 with average about 0.25. The magmatic eU/eTh ratio is about 0.33, then in monzogranites this ratio is relatively decreased than magmatic ratio, indicating that, the relatively depleting of uranium in the monzogranites rocks. The uranium mobilization $\text{eUm} = (\text{eU} - \text{eTh} / 3.5)$ of monzogranites rocks range from -2.1 to 0.7 with an average of about -1.7. These negative value of eUm indicating also the migration of uranium out the monzogranite rocks..(Table 3).

Table 3: The range and average of D. R., K%, eU, eTh and eU/eTh of monzogranites, syenogranites and shear zone of Gabal Rabdi area, South Eastern Desert, Egypt

Rock types		D.R.(nSvh ⁻¹)	K%	eU	eTh	eU/eTh	eUm
Monzogranites (N=18)	Max.	279	6	9	32	0.33	0.7
	Min.	190	4.3	4	19	0.19	-2.1
	Average	240	5.4	7	25	0.25	-1.7
Syenogranites (N=16)	Max.	320	6.4	14	29	0.41	3.6
	Min.	180	3.9	6	16	0.28	-0.2
	Average	245	4.8	9	23	0.37	1.5
Shear zone (N=17)	Max.	965	4.8	98	49	2.2	85
	Min.	386	3.1	11	20	0.37	2.2
	Average	660	3.8	36	28	1.1	26.5

In syenogranites the eU contents range from 6 to 14 ppm with an average of about 9 ppm. The eTh contents range between 16 to 29 ppm with an average of about 23 ppm. The eU/eTh ratio ranges between 0.28 to 0.41 with an average of about 0.37. The magmatic eU/eTh ratio is about 0.33, then in syenogranites this ratio is relatively increased than the magmatic ratio, indicating that the relatively enrichment of uranium in the monzogranites rocks. The uranium mobilization $eUm = (eU - eTh/3.5)$ of syenogranites range from -0.2 to 3.6 with an average about 1.5. These positive values indicate uranium addition by mobilization into the syenogranites. (Table 3).

In tsyenogranite shear zone the eU contents range from 5 to 98 ppm with an average of about 36 ppm. The eTh contents range between 20 to 49 ppm with an average of about 28 ppm. The eU/eTh ratio ranges between 0.37 to 2.2 with an average of about 1.1. The magmatic eU/eTh ratio is about 0.33, then in the shear zone the ratio is more than the magmatic ratio, indicating the enrichment of uranium in the shear zone. The uranium mobilization $eUm = (eU - eTh/3.5)$ of the shear zone range from 2.2 to 85 with an average of

about 26.5. This positive value of eUm indicates uranium addition by mobilization into the shear zone (Table 3).

The radioactivity of monzogranites and syenogranites are related to magmatic origin, while in the shear zone, the presence of radioactive anomalies are related to structure control, leaching and secondary hydrothermal solutions. The structure controlling presence of radioactive anomalies include strike slip faults, joints and shear zone, which acts as path ways to uranium solutions. The leaching mean that the uranium has been leached from other surrounding rocks to the place of mineralization transported, by means of circulating ground water and finally deposited in its present location, i.e. the source of uranium specially in the shear zone may coming by leaching of surrounding rocks specially granitic rocks as well as by hydrothermal ascending solutions.

The variation diagrams of the monzogranite rocks, (Figs. 31-33) showing a weakly relation between eU vs eTh, but they show positive relations between eU vs. eU/eTh, and negative relation between eU/eTh vs. eTh. These relations indicating that the eU contents suffered leaching out the monzogranites rocks.

The variation diagrams of the syenogranites rocks, (Figs.34-36) showing a positive relation between eU vs eTh, but they show a weakly positive relation between eU vs. eU/eTh, and a weakly negative relation between eU/eTh vs. eTh. These relations indicating that all measurements of eU suffered weakly enrichment due to hydrothermal solutions as well as by leaching from surrounding rocks.

The variation diagrams of the shear zone, (Figs.37 -39) showing a positive relation between eU vs eTh, eU vs. eU/eTh, and eU/eTh vs. eTh. These relations indicate that, in shear zone the uranium had been highly enrichment by leaching of uranium as well as by hydrothermal solutions which rich also in thorium.

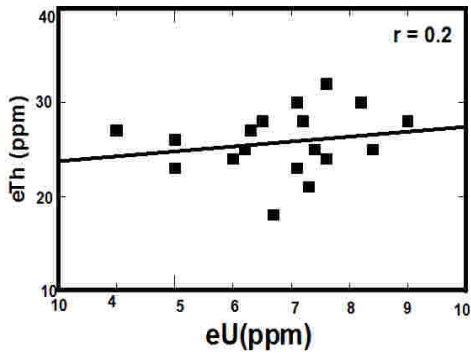


Fig. 31: The relations between eU vs. eTh in monzogranites

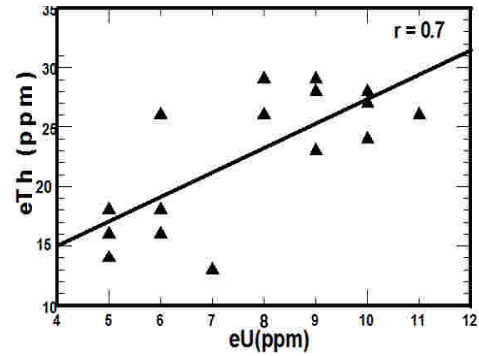


Fig. 34: The relations between eU vs. eTh in syenogranites

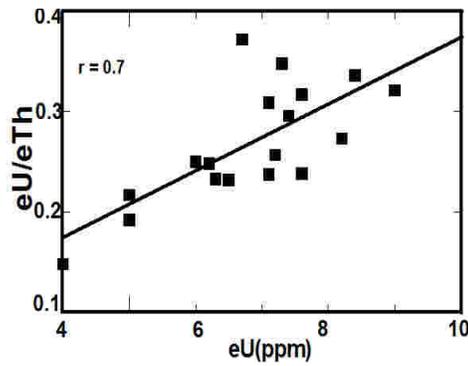


Fig. 32: The relations between eU vs. eU/eTh in monzogranites

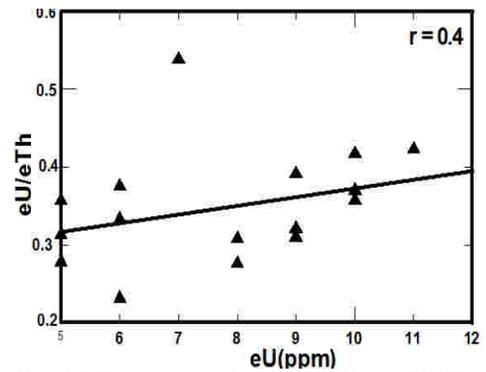


Fig. 35: The relations between eU vs. eU/eTh in syenogranites

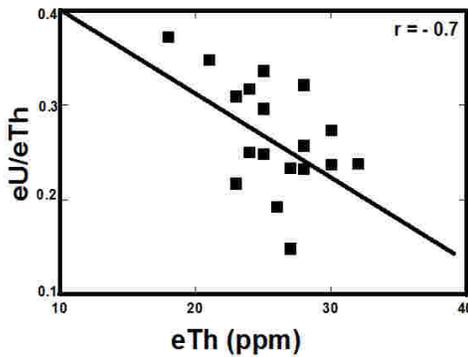


Fig. 33: The relations between eTh vs. eU/eTh in monzogranites

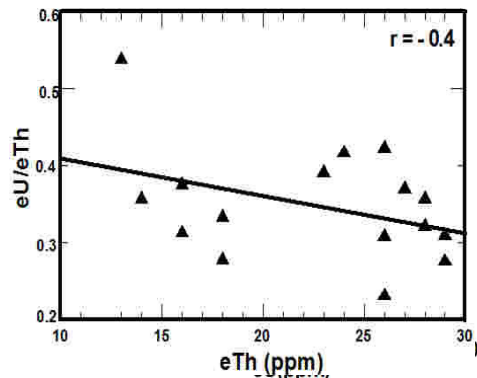


Fig. 36: The relations between eTh vs. eU/eTh in syenogranites

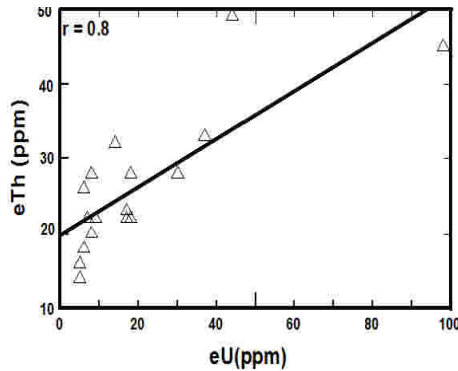


Fig. 37 :The relations between eU vs. eTh in the shear zone in syenogranites

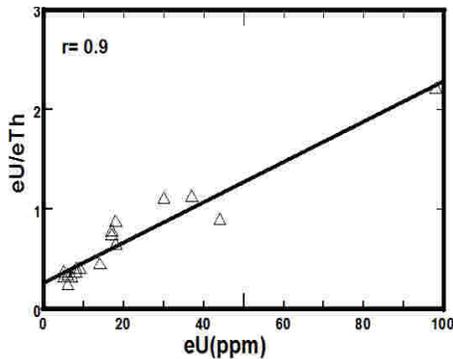


Fig. 38 :The relations between eU vs. eU/eTh in the shear zone in syenogranites

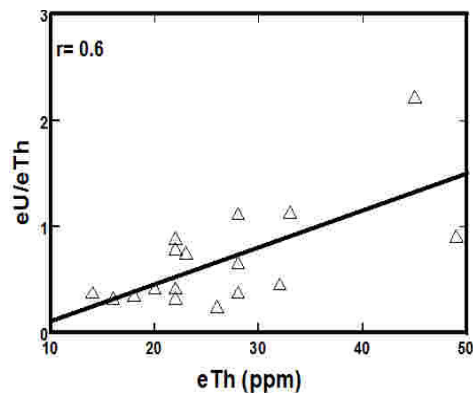


Fig. 39 :The relations between eTh vs. eU/eTh in the shear zone in syenogranites

CONCLUSIONS

1-Gabal Rabdi area is located in south Eastern Desert of Egypt between Lat. $24^{\circ} 55' 28'' - 24^{\circ} 57' 27''$ N and Long. $34^{\circ} 46' 34'' - 34^{\circ} 50' 39''$ E. The basement rocks in the study area are metavolcanics, younger gabbros intruded by younger granites and extruded by post granitic dykes.

2-The younger granites are represented as monzogranites and syenogranites

3- Structurally, the study area was subjected to two strike slip faults in NW-SE and NE-SW directions.

4- According to effect of this structure, the granitic rocks (especially syenogranites) are highly fractured, sheared (due to presence of shear zone) and also affected by later solutions leading to hematitization proces. In syenogranites, the presence of cracked crystals and strongly undulatory quartz, all these features point to subsolidus deformation (Patterson et al., 1989).

5-The monzogranites are composed mainly of quartz, potash feldspars, plagioclase, biotite and hornblende. Allanit, zircon and opaques (iron oxides and pyrite) are accessories, while the syenogranites are composed mainly of potash feldspars, quartz, plagioclase, biotite and muscovite. Zircon and opaques (iron oxides and pyrite) are accessories.

6- Geochemically, the monzogranites are considered as I-type, originated from metaluminous calc-alkaline magma and formed under an extensional regime. They are crystallized at temperature $< 800^{\circ}\text{C}$, with pressure between 2 to 4 kb. On the other hand syenogranites are related to A-type, originated from peraluminous calc-alkaline magma. They are post-orogenic, formed under an extensional regime and crystallized at temperature $< 800^{\circ}\text{C}$ with pressure from 1 to 3 kb.

7- Mineralogically, the younger granites are characterized by presence of columbite, pyrite, zircon and allanite while radioactive

mineral (uranophane) related to the shear zone.

8- Spectrometry, the monzogranites have an average equal to 7 ppm eU content and 25 ppm eTh content with an average eU/eTh ratio equal 0.25. The syenogranites have an average equal to 9 ppm eU content and 23 ppm eTh content with an average of eU/eTh ratio equal 0.37. The shear zone in syenogranites, gives the highly radioactive point, due to presence of uranophane mineral, with eU contents up to 98 ppm.

9- The origin of uranium in the shear zone is epigenetic related to leaching from surrounding rocks and from ascending hydrothermal solutions which moved along strike slip faults, joints and shear zone, which acts as path ways to uranium solutions.

REFERENCES

- Abdel-Rahman, A.M., and Martin, R.F., 1990. The mount Gharib A-type granite Nubian Shield: petrogenesis and role of metasomatism at the source. *Contribution mineralogy petrology*, 104, 173-183.
- Akaad, M.K., and Noweir, A.M., 1980. Geology and lithostratigraphy of the Arabian Desert orogenic belt of Egypt between latitudes 25 35 E and 26 30 N. *Inst. Appl. Geol. (Jaddah), Bull. 3, 4*, 127-134.
- Ali, M.A.; Moussa, E.M.M., and Darwish, M.E., 2005. Petrochemistry and radioactivity of the younger granites at Gabal Rabad, south Eastern Desert, Egypt. 4th Inter. Conf. Geol. Africa, 1, 393-402.
- Barker, F., 1979. Trondhjemites definition, environment and hypotheses of origin. In: *Trondhjemites, dacites and related rocks* (Barker, Ed.). *Developments in petrology*, El Sevier Publish. Co., Amsterdam, 6, 1-12.
- Batchelor, R.A., and Bowden, P., 1985. Petrogenetic interpretation of granitoid rock series using multication parameters. *Chem. Geol.*, 48, 43-55.
- Bucanan, M.S., 1982: The geochemistry of some igneous rocks. *Geochim cosmo-chem. Acta*, 9, 297- 308
- Clark, S.P.Gr.; Peterman, J.E., and Heier, K.S., 1966. Abundance of U, Th and K. In: *Handbook of physical constants* (Clark, S. P. Jr., Ed.). *Mem. Geol. Soc. Am.* , 97, 587.
- Eby, G.N., 1992. Chemical subdivision of the A-type granitoids: Petrogenesis and tectonic implications, *Geology*, 20, 641-644.
- El Gaby, S., and Habib, M.S., 1982. Geology of the area south west of Port Safaga with special emphasis on the granitic rocks. *Eastern Desert, Egypt. Ann. Geol. Surv.Egypt.*, 12, 47-71.
- EL Gaby, S.; List, F.K., and Tehrani, R., 1990. The basement complex of the Eastern Desert and Sinai. In: *The geology of Egypt* (Said, R., Ed.). Balkema, Rotterdam, Brookfield, 175-184.
- Falkum, T., and Rose-Hansen, J., 1978. The application of the radioelement studies in solving petrological problems of the Precambrian intrusive Homme granite in the Flekkefjord area, South Norway. *Geol.*, 239, 73-86.
- Ibrahim, M.E., 1996. Petrochemical investigations on Magal Gebriel uraniferous granites, South Eastern Desert, Egypt, *Egypt. Acad. Sc.*, 46, 587-601.
- Irvine, T.N., and Baragar, W.R.A., 1971. A guide to the chemical classification of the common volcanic rocks. *Canad. J. earth Sci.*, 8, 523-548.
- Le Maitre, R.W., 1989. A classification of igneous rocks of terms. Blackwell, Sci. Bull. Oxford, London, 171.
- Maniar, P.D., and Piccoli, P.M., 1989. Tectonic discrimination of granitoids. *Geol. Soc. Am. Bull.*, 101, 635-643.
- Mason, D., 1966. *Principals of geochemistry*. 3rd Edition, Jhon Wiley and Sons, New York, 310 .
- Newberry R.J.; Burns, L.E.; Swanson, S.E., and Smith, T.E., 1990. Comparative petrologic evolution of the Sn and W granites of the Fairbanks-

- Circle area, interior Alaska. In: Ore-bearing granite systems; petrogenesis and mineralizing processes (Stein,HJ., and Hannah,JL., Eds.). Geol. Society of America Special Paper, 121-142.
- Noweir, A.M.; Sewifi, B.M., and Abu El Ela, A. M., 1990. Geology, petrology and petrogenesis of the Egyptian younger granites. Qatar Univ. Sci. Bull, 10, 363-393.
- Paterson, S.R.; Vernon, R.H., and Tobisch, O.H., 1989. Preview of criteria for the identification of magmatic and tectonic foliations in granitoids. J. structural Geol., 11, 340-363.
- Petro, W.L.; Vogal, T.A., and Wilbant, J.T., 1979. Major element chemistry of plutonic rock suites from comprassional and extensional plate boundaries. Chem. Geol. , 26, 217-235.
- Ragab, A.I.; Menesy, M.Y., and Diab, M.M., 1989. Petrology and petrogenesis of the Older and Younger Granitoids of Wadi Beizah area, Central Eastern Desert, Egypt. J. Afri. Earth Sci., 9, 303-315.
- Ragland, P.C.; Billing G.K., and Adams, J.A.S., 1967. Chemical fractionation and its relationship to the distribution of thorium and uranium in zoned granite batholiths. Geochem. Cosmochem. Acta, 31, 17-33.
- Rogers, J.J.W., and Adams, J.S.S., 1969. Uranium In: Handbook of geochemistry (Wedepohl, K. H., Ed). New York , Springer- Ver- Lag,4, B1-92. C10, 92.
- Stern, R.J., and Hedge, CE., 1985. Geochronological and isotopic constraints on Late Precambrian crustal evolution in the Eastern Desert of Egypt. Am. J. Sci., 285, 97-127.
- Streckeisen, A.L., 1976. To each plutonic rock its proper name, Earth Sci. Rev., 12, 1-33.
- Tischendorf, G. ,1977. Geochemical and petrographic characteristic of silicic magmatic rocks associated with rare-element mineralization: in mineralization associated with acid magmatism / stemprok, M. Burnol, L. and Tischendorf, G. Eds., 2, 41-96.
- Tuttle, O.F., and Bowen , N.L., 1958. Origin of granites in the light of experimental studies in the system $\text{NaAlSi}_3\text{O}_8$ - KAlSi_3O_8 - SiO_2 - H_2O . Geol. Soci. Amer. Memoir, 74, 1-153.

جيولوجية وجيوكيميائية وتمعدنات الجرانيتات الحديثة بمنطقة جبل رابدى, جنوب الصحراء الشرقية, مصر

محمد عبدالله راشد

تقع منطقة جبل رابدى في جنوب الصحراء الشرقية و تبعد حوالي ٢٠ كم جنوب- غرب مدينة مرسى علم. منطقة الدراسة تتكون من صخور البركانيات القديمة وصخور الجابرو الحديثة ثم صخور الجرانيتات الحديثة وصخور المنطقة جميعها مقطوعة بمجموعة من القواطع. وقد اختص هذا البحث بدراسة الصخور الجرانيتية الحديثة حيث أمكن تقسيمها إلى المونزوجرانيت و السيانوجرانيت. تنتمي صخور المونزوجرانيت إلى النوع (I) ذات خواص ميتالومينية نشأت من صهارة ذات طبيعة كلس-قلوية و نشأت هذه الصخور في بيئة شد تكتونية عند درجة حرارة أعلى من ثمانمائة درجة مئوية و تحت ضغط من اثنين إلى أربعة كيلو بار. فى حين تنتمي صخور السيانوجرانيت إلى النوع (A) ذات خواص فوق الومينية نشأت من صهارة ذات طبيعة كلس-قلوية و نشأت هذه الصخور في بيئة شد تكتونية عند درجة حرارة اقل من ثمانمائة درجة مئوية تحت ضغط من واحد إلى ثلاثة كيلو بار . أظهرت

الدراسة المعدنية لهذه الجرانيتات احتوائها على معادن اليورانيوم و الكولمبيت والبيريت و الزيركون والالانيت. كما أظهرت الدراسة الإشعاعية وجود بعض الشاذات الإشعاعية مرتبطة بنطاق القص الموجود بالسيانوجرانيت حيث يصل محتوى اليورانيوم ل ٩٨ جزء في المليون و يعزى مصدر اليورانيوم بنطاق القص إلى المحاليل الحارة المساعدة وكذلك اليورانيوم المنقول من الصخور المجاورة ثم ترسب في نطاق القص.